# Extending the G2++ model: fitting the term structure of implied volatility*

Mario Bonino†, Riccardo Casalini‡

May 30, 2020

**Abstract**

This paper describes a fast and robust procedure for calibrating a two factor Gaussian model (G2++) with piecewise-constant volatility to a large set of options on interest rates swaps. As far as we know the algorithm implemented is novel as it overcomes some issues affecting highly parameterized models like model identification and the need to employ heuristic optimizations in order to get a good overall fitting. In this sense, our procedure extends the G2++ model ability to reproduce the term structure of volatility implied by interest rate options, similarly to how the Hull and White model extended the Vasicek model in order to perfectly fit the term structure of interest rates.

***Keywords:*** Interest Rate Risk, Gaussian Term Structure Model, G2++, Implied Volatility, Swaptions, Monte Carlo simulations

## 1 Introduction

> Gaussian models like the G2++ model are very useful in practice, despite their unpleasant feature of the theoretical possibility of negative rates.
> — Damiano Brigo, Fabio Mercurio. *Interest Rate Models – Theory and Practice, Section 4.2*

Gaussian models have always been attractive because of their analytical

*The opinions and views reported in this paper belong exclusively to the authors and don't necessarily reflect the opinions and views of the company they work for.

†Risk Management, UnipolSai Assicurazioni, e-mail: Mario.Bonino@unipolsai.it

‡Risk Management, Unipolsai Assicurazioni, e-mail: Riccardo.Casalini@unipolsai.it



Electronic copy available at: https://ssrn.com/abstract=3598285

tractability. However, until recent years, the possibility of allowing negative rates has been considered a drawback of these models. Today, this shortcoming has become a selling point, since interest rates have been negative for some time, but this is not the only aspect that makes them interesting.

This paper deals with a specific member of the family of Gaussian models, more precisely the one which is conventionally known as G2++. This model is a two factors evolution of the popular one factor Hull-White model (see [11]), which in turn was an extension of the Vasicek model (see [13]). Like the latter, this is a model of the continuously compounded, or instantaneous, short rate, whose dynamic is characterized by mean reversion. Like the former, it is a "no-arbitrage" model in the sense that it perfectly reproduces the term structure of interests rates at inception. Because the Hull-White model extends the ability of the Vasicek model to fit the initial interest rates term structure, it is also called "extended Vasicek" model.

In this paper, we apply the same idea to the volatility of the short rate, which we allow to vary with time, so that this is no longer time-homogeneous. By doing so, we improve the ability of the classical G2++ model to reproduce the prices of options on interest rates, such as caps and floors, or swaptions (options on interest rate swaps). In particular, we will show that, utilizing a particular procedure, the G2++ model can be extended (in the sense specified above), so that it can be accurately calibrated on a very large number of swaptions, without making use of heuristic optimizations to identify the model, in spite of the high number of parameters that have to be determined. The calibrated model will convey the information on the term structure of the volatility in a deterministic, piecewise-constant, function of time.

We think that this approach has interesting applications. Obviously, it can be used to price interest rate derivatives and securities with embedded optionality, such as callable (or puttable) bonds, or structured products, like Constant Maturity Swaps (or "CMS"). Because the analytical tractability of the original G2++ model is retained by the extended version described in this paper, the G2++ model with piecewise-constant volatility can be used very effectively in conjunction with credit spread models and equity models in (risk-neutral) Monte Carlo simulations. For example, reduced-form credit spread models where the credit risk is modelled by means of an instantaneous hazard rate, may have a similar analytical tractability and therefore, can be specified quite naturally in conjunction with instantaneous short rate models[1].

[1]See in particular [5] for a discussion on reduced-form credit models based on instantaneous hazard rate; an application to insurance products of a multi-factor risk set-up which makes use of affine term structure models can be found in [7] and in [8]



Electronic copy available at: https://ssrn.com/abstract=3598285

Moreover, it is worth mentioning that instantaneous short rate models are very popular among econometricians, to a point they can be considered a benchmark for real-world term structure models[2]. Although our extended G2++ is a risk-neutral model, nothing prevents to apply it on data generated from a real-world model. This is the case in regulatory capital evaluations, which typically require that a number of risk-neutral runs are performed over a set of real-world economic scenarios, which can be few in case of stress tests, or many when the official Solvency Capital Requirement has to be evaluated by an insurance company[3]. In those cases, it may be sensible to use models that maintain a similar behavior moving from the real-world to the risk-neutral measure. Eventually, one reason for the higher popularity of other models in options pricing, is that a pure Gaussian dynamic of interest rates is not consistent with "smiles" observed in option prices[4]. Nevertheless, this limitation could be less binding in less specialized contexts and, possibly, it may be bridged using a mixture of Gaussian distributions as in [4]. This latter topic could be the subject of future research.

The paper is structured as follows. In section 2 the piecewise-constant volatility extension of the G2++ model, or XG2++ for brevity, is introduced. In section 3 the algorithm that we have adopted for calibrating the model is described and some results are reported. The fact that the calibration procedure uses a deterministic optimization algorithm and needs little or no human supervision makes, in our opinion, this approach interesting. Eventually, in the appendix we have dedicated more room for the most involved mathematical passages.

# 2 The model

## 2.1 The time-independent formulation

We assume the existence of a sample space $\Omega$, equipped with a $\sigma$-algebra $\mathcal{F}$, on which the risk-neutral probability measure $\mathbb{Q}$ is defined. There exists a

[2] See [2]

[3] Actually, the Solvency II directive requires insurance companies too calculate every year their Solvency Capital Requirement as the unexpected loss occurring with 99.5% confidence on their Basic Own Funds, the latter being the net value of their assets and liabilities evaluated on a one-year horizon. The evaluation of assets and liabilities at the one-year horizon has to be "market consistent", which translates: the pricing of assets and liabilities has to be done under the Risk Neutral measure.

[4] Papers on this topics are too many to provide a comprehensive list. Therefore, we mention only few classics: [6], [10] and [9].



Electronic copy available at: https://ssrn.com/abstract=3598285

bank account asset, denoted by $(B(t))_{t\geq 0}$, which satisfies

$$dB(t) = r(t)B(t)dt, \quad B(0) = 1$$

where $(r(t))_{t\geq 0}$ is the risk-free short rate. Moreover, we assume the existence of a liquid zero-coupon bond market, i.e. we assume the existence of a tradable zero-coupon bond at every instant $s$ for each maturity $t > s$. We denote the (stochastic) price of that bond with $P(s,t)$. The relation $P(t,t) = 1$ holds for all $t$.

Following [3], we assume that the risk-neutral dynamics of the risk-free rate in the G2++ model is given by

$$r(t) = x(t) + y(t) + \varphi(t), \qquad r(0) = r_0$$

where $r_0 \in \mathbb{R}$, $\varphi$ is a deterministic function defined on $[0, T^*]$ for $T^* > 0$ and the processes $(x(t))_{t\geq 0}, (y(t))_{t\geq 0}$ satisfy the following stochastic differential equations

$$\begin{aligned} dx(t) &= -ax(t)dt + \sigma dW_1(t), \qquad x(0) = 0 \\ dy(t) &= -by(t)dt + \eta dW_2(t), \qquad y(0) = 0 \end{aligned}$$

where $a, b, \sigma, \eta \in \mathbb{R}^+$ and $(W_1(t), W_2(t))$ is a 2-dimensional $\mathbb{Q}$-Brownian motion with instantaneous correlation given by

$$dW_1(t)dW_2(t) = \rho \; dt$$

with $\rho \in \mathbb{R}$ and $-1 \leq \rho \leq 1$. We introduce $(\mathcal{F}_t)_{t\geq 0}$ as the filtration generated by the processes $(x(t))_{t\geq 0}, (y(t))_{t\geq 0}$. We assume that $(\Omega, \mathcal{F}, (\mathcal{F}_t)_{t\geq 0}, \mathbb{Q})$ is a standard filtered probability space.

Since $(x(t))_{t\geq 0}, (y(t))_{t\geq 0}$ are Ornstein-Uhlenbeck processes, given $0 < s < t$, conditional on $\mathcal{F}_s$, the short-rate $r(t)$ is given by

$$\begin{aligned} r(t) =& x(s)e^{-a(t-s)} + y(s)e^{-b(t-s)} \\ &+ \sigma \int_s^t e^{-\sigma(t-u)} dW_1(u) + \eta \int_s^t e^{-\eta(t-u)} dW_2(u) + \varphi(t) \end{aligned}$$

## 2.2 The piecewise-constant parameters formulation

In order to accommodate more general volatility structures, the model can be specified with piecewise-constant (PC) volatility parameters $(\sigma, \eta)$. More precisely, we assume that the processes $(x(t))_{t\geq 0}, (y(t))_{t\geq 0}$ satisfy the following stochastic differential equations

$$dx(t) = -ax(t)dt + \sigma(t)dW_1(t), \qquad x(0) = 0$$



Electronic copy available at: https://ssrn.com/abstract=3598285

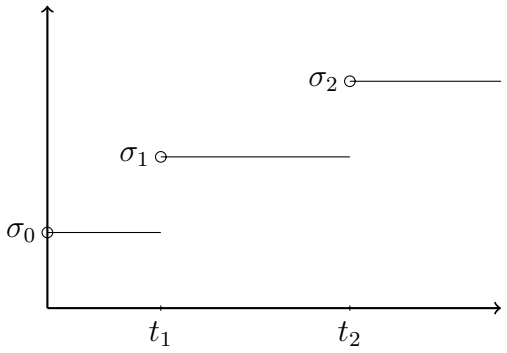


Figure 1: Example of a piecewise-constant $\sigma$ function.

$$dy(t) = -by(t)dt + \eta(t)dW_2(t), \qquad y(0) = 0$$

where the functions $(\sigma, \eta)$ are right-continuous piecewise-constant, i.e. there exist $n$ jump times $t_1, \ldots, t_n$, positive constants $\sigma_0, \sigma_1, \ldots, \sigma_n$ and $\eta_0, \eta_1, \ldots, \eta_n$, such that

$$\sigma(t) = \sum_{i=0}^{n} \sigma_i \chi_{[t_i, t_{i+1})}, \quad \eta(t) = \sum_{i=0}^{n} \eta_i \chi_{[t_i, t_{i+1})}$$

with the agreement that $t_0 = 0$ and $t_{n+1} = +\infty$. An example of such a function can be seen in Figure 1[5].

## 2.3 Main results

In this section, we provide some G2++ results, according to the piecewise-constant specification. This section and the next are based on section 4.2 of [3].

When performing calculations in the piecewise-constant setting, one often finds integrals involving piecewise-constant functions. Therefore, it is useful to analyze in detail how to correctly carry out these calculations.

For example, the solution of a standard Ornstein-Uhlenbeck SDE

$$dx(t) = -ax(t)dt + \sigma dW(t)$$

is, for $t > s$,

$$x(t) = x(s)e^{-a(t-s)} + \int_s^t \sigma e^{-a(t-u)} dW(u)$$

If the SDE has a piecewise-constant volatility function, we will get

$$x(t) = x(s)e^{-a(t-s)} + \int_s^t \sigma(u) e^{-a(t-u)} dW(u)$$

[5]Notice that the jump times of the two functions are the same.



Electronic copy available at: https://ssrn.com/abstract=3598285

Now, the volatility function is constant between jump times, therefore the integral will break into the sum of sub-integrals between the jump times in the interval $[s,t]$. In other words, the integral will look like

$$\begin{aligned}\int_s^t \sigma(u)e^{-a(t-u)}dW(u) = \sigma_{i^*-1}\int_s^{t_{i^*}} e^{-a(t-u)}dW(u)\\ + \sigma_{i^*}\int_{t_{i^*}}^{t_{i^*+1}} e^{-a(t-u)}dW(u)\\ + \dots\\ + \sigma_{j^*}\int_{t_{j^*}}^{t} e^{-a(t-u)}dW(u)\end{aligned}$$

for some $i^*$ and $j^*$. It is helpful to introduce some terminology to easily denote the sub-intervals and their extreme points.

**Definition 1.** Given a right-continuous piecewise-constant (p.c.) function $\sigma$, identified by $n$ jump times $t_1,\dots,t_n$ and positive constants $\sigma_0,\sigma_1,\dots,\sigma_n$, such that

$$\sigma(t) = \sum_{i=0}^{n} \sigma_i \chi_{[t_i,t_{i+1})}$$

given a time $s>0$, we denote by $i(s)$ the first jump-time after $s$, i.e.

$$i(s) = \min\{i\in\mathbb{N} : t_i \geq s\}$$

If no jump occurs after $s$, i.e. $\{i\in\mathbb{N} : t_i\geq s\} = \emptyset$, we put $i(s) = n+1$.

According to the particular structure of the volatility function, the Ornstein-Uhlenbeck equation becomes

$$\begin{aligned}x(t) &= x(s)e^{-a(t-s)} + \int_s^t \sigma(u)e^{-a(t-u)}dW(u)\\ &= x(s)e^{-a(t-s)} + \sigma_{i(s)-1}\int_s^{t_{i(s)}} e^{-a(t-u)}dW(u)\\ &\quad + \sigma_{i(s)}\int_{t_{i(s)}}^{t_{i(s)+1}} e^{-a(t-u)}dW(u) + \dots\\ &\quad + \sigma_{i(t)-1}\int_{t_{i(t)-1}}^{t} e^{-a(t-u)}dW(u)\\ &= x(s)e^{-a(t-s)} + \sum_{i=i(s)}^{i(t)} \sigma_{i-1}\int_{\max(s,t_{i-1})}^{\min(t,t_i)} e^{-a(t-u)}dW(u)\end{aligned}$$

The discussion above justify the following proposition.



Electronic copy available at: https://ssrn.com/abstract=3598285

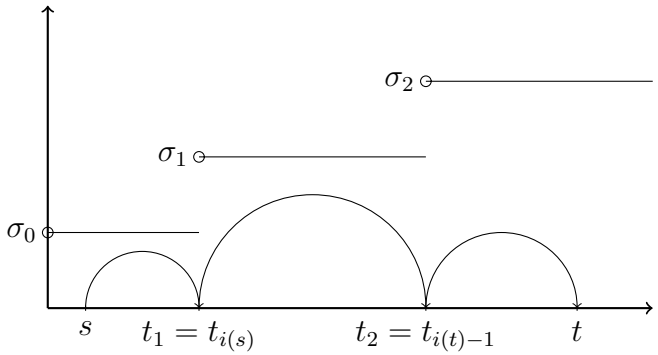


Figure 2: Example of a piecewise-constant $\sigma$ function. The arcs illustrate the integration sub-intervals from $s$ to $t$.

**Proposition 1.** *The short-rate in the piecewise-constant volatility formulation, conditionally on $\mathcal{F}_s$, is given by*

$$\begin{aligned} r(t) = \varphi(t) + x(s)e^{-a(t-s)} + y(s)e^{-a(t-s)} \\ + \sum_{i=i(s)}^{i(t)} \sigma_{i-1} \int_{\max(s,t_{i-1})}^{\min(t,t_i)} e^{-a(t-u)} dW_1(u) \\ + \sum_{i=i(s)}^{i(t)} \eta_{i-1} \int_{\max(s,t_{i-1})}^{\min(t,t_i)} e^{-b(t-u)} dW_2(u) \end{aligned}$$

*Proof.* We just need to consider the solution of the SDE of $(x(t))_{t\geq 0}$ (the solution of $(y(t))_{t\geq 0}$ is analogous) given above and remember that $r(t) = x(t) + y(t) + \varphi(t)$. □

Proposition 1 lets us prove the following result.

**Proposition 2.** *The short-rate in the piecewise-constant volatility formulation, conditionally on $\mathcal{F}_s$, is a normal random variable, with mean and variance given by*

$$\mathbb{E}\left[r(t)|\mathcal{F}_s\right] = \varphi(t) + x(s)e^{-a(t-s)} + y(s)e^{-a(t-s)}$$

$$\begin{aligned} \mathbb{V}\left[r(t)|\mathcal{F}_s\right] = \sum_{i=i(s)}^{i(t)} \left[ \frac{\sigma_{i-1}^2}{2a} \left( e^{-2a\Delta t_i^{(r)}} - e^{-2a\Delta t_i^{(l)}} \right) \right. \\ \left. + \sum_{i=i(s)}^{i(t)} \frac{\eta_{i-1}^2}{2b} \left( e^{-2b\Delta t_i^{(r)}} - e^{-2b\Delta t_i^{(l)}} \right) + \sum_{i=i(s)}^{i(t)} \frac{2\rho\sigma_{i-1}\eta_{i-1}}{a+b} \left( e^{-(a+b)\Delta t_i^{(r)}} - e^{-(a+b)\Delta t_i^{(l)}} \right) \right] \end{aligned}$$



Electronic copy available at: https://ssrn.com/abstract=3598285

*where*

$$\Delta t_i^{(l)} := t - \max(s, t_{i-1}), \qquad \Delta t_i^{(r)} := t - \min(t, t_i)$$

*Proof.* See Appendix A.1. □

Since the price of a zero-coupon bond is given by[6]

$$P(s,t) = \mathbb{E}^{\mathbb{Q}}\left[\exp^{-\int_s^t r(u)du} | \mathcal{F}_s\right]$$

it is important to know, if possible, the distribution of $\int_s^t r(u)du$. The following Proposition specifies that.

**Proposition 3.** *The integrated process $I(s,t) := \int_s^t r(u)du$ is, conditional on $\mathcal{F}_s$, normal with mean given by*

$$M(s,t) := \mathbb{E}\left[I(s,t)|\mathcal{F}_s\right] = \int_s^t \varphi(u)du + x(s)\frac{1-e^{-a(t-s)}}{a} + y(s)\frac{1-e^{-b(t-s)}}{b}$$

*and variance equal to*

$$V(s,t) := \mathbb{V}\left[I(s,t)|\mathcal{F}_s\right] =$$
$$\sum_{i=i(s)}^{i(t)} \left\{ \frac{\sigma_{i-1}^2}{a^2}\left[\left(\Delta t_i^{(l)} - \Delta t_i^{(r)}\right) - \frac{2}{a}\left(e^{-a\Delta t_i^{(r)}} - e^{-a\Delta t_i^{(l)}}\right) + \frac{1}{2a}\left(e^{-2a\Delta t_i^{(r)}} - e^{-2a\Delta t_i^{(l)}}\right)\right]\right.$$
$$+\frac{\eta_{i-1}^2}{b^2}\left[\left(\Delta t_i^{(l)} - \Delta t_i^{(r)}\right) - \frac{2}{b}\left(e^{-b\Delta t_i^{(r)}} - e^{-b\Delta t_i^{(l)}}\right) + \frac{1}{2b}\left(e^{-2b\Delta t_i^{(r)}} - e^{-2b\Delta t_i^{(l)}}\right)\right]$$
$$+\frac{2\rho\sigma_{i-1}\eta_{i-1}}{ab}\left[\left(\Delta t_i^{(l)} - \Delta t_i^{(r)}\right) - \frac{1}{a}\left(e^{-a\Delta t_i^{(r)}} - e^{-a\Delta t_i^{(l)}}\right) - \frac{1}{b}\left(e^{-b\Delta t_i^{(r)}} - e^{-b\Delta t_i^{(l)}}\right)\right.$$
$$\left.\left. + \frac{1}{a+b}\left(e^{-(a+b)\Delta t_i^{(r)}} - e^{-(a+b)\Delta t_i^{(l)}}\right)\right]\right\}$$

*where $\Delta t_i^{(l)}$ and $\Delta t_i^{(r)}$ are as in Proposition 2*

*Proof.* See Appendix A.2. □

**Corollary 1.** *The price of a zero-coupon bond at time $t$, conditional on $\mathcal{F}_s$, with $s < t$, is given by*

$$P(s,t) = \exp\left[-M(s,t) + \frac{1}{2}V(s,t)\right]$$

[6] See [1], Chapter 23 (Short Rate Models).



Electronic copy available at: https://ssrn.com/abstract=3598285

*Proof.* Using Proposition 3, conditional on $\mathcal{F}_s$, the random variable

$$\exp\left[-\int_s^t r(u)\ du\right]$$

is log-normal. Remembering that, if $Z$ is a normal random variable with mean and variance given by $m$ and $\sigma^2$, the expected value of $\exp(Z)$ is $\exp(m + \frac{1}{2}\sigma^2)$. □

The following Proposition shows that it is not necessary to actually calculate the $\varphi$ function, because only its integral is needed.

**Proposition 4.** *To achieve the perfect fitting at time $t = 0$ of the initial term structure of interest rates, the $\varphi$ function must satisfy*

$$\exp\left[-\int_s^t \varphi(u)\ du\right] = \frac{P(0,t)}{P(0,s)} \exp\left\{-\frac{1}{2}\left[V(0,t) - V(0,s)\right]\right\}$$

*Proof.* By Corollary 1,

$$P(0,t) = \exp\left[-M(0,t) + \frac{1}{2}V(0,t)\right] = \exp\left[-\int_0^t \varphi(u)du + \frac{1}{2}V(0,t)\right]$$

So,

$$\exp\left[-\int_0^t \varphi(u)du\right] = P(0,t)\exp\left[-\frac{1}{2}V(0,t)\right]$$

and also

$$\exp\left[-\int_0^s \varphi(u)du\right] = P(0,s)\exp\left[-\frac{1}{2}V(0,s)\right]$$

Therefore,

$$\exp\left[-\int_s^t \varphi(u)\ du\right] = \frac{P(0,t)}{P(0,s)} \exp\left\{-\frac{1}{2}\left[V(0,t) - V(0,s)\right]\right\}$$

□

Finally, we are able to express the zero-coupon bond price in terms of the initial term structure and model parameters only.

**Theorem 1** (Zero-coupon bond price)**.** *The price of a zero-coupon bond at time $t$, conditional on $\mathcal{F}_s$, with $s < t$, is given by*

$$P(s,t) = \frac{P(0,t)}{P(0,s)} \exp\left\{\frac{1}{2}\left[V(s,t) - V(0,t) + V(0,s)\right]\right.$$
$$\left. -\frac{1-e^{-a(t-s)}}{a}x(s) - \frac{1-e^{-b(t-s)}}{b}y(s)\right\}$$



Electronic copy available at: https://ssrn.com/abstract=3598285

Now, we introduce the *forward measure*, which will be useful in pricing derivatives such as swaptions.

**Definition 2** (Forward measure)**.** The forward measure $\mathbb{Q}^T$ is the probability measure associated with the zero-coupon bond that expires at time $T$ as numeraire. In other words, the Radon-Nikodym derivative of $\mathbb{Q}^T$ with respect to $\mathbb{Q}$ is given by[7],

$$\frac{d\mathbb{Q}^T}{d\mathbb{Q}} = \frac{B(0)}{B(T)}\frac{P(T,T)}{P(0,T)} = \exp\left\{-\frac{1}{2}V(0,T) - \int_0^T [x(u) + y(u)\ du]\right\}$$

The following Proposition describes the dynamics of $x(t)$ and $y(t)$ under $\mathbb{Q}^T$.

**Proposition 5.** *The processes $x(t)$ and $y(t)$ obey the following $\mathbb{Q}^T$-dynamics*

$$dx(t) = \left[-ax(t) - \sigma(t)^2\left(\frac{1-e^{-a(T-t)}}{a}\right) - \rho\eta(t)\sigma(t)\left(\frac{1-e^{-b(T-t)}}{b}\right)\right]dt + \sigma(t)dW_1^T(t)$$

$$dy(t) = \left[-by(t) - \eta(t)^2\left(\frac{1-e^{-b(T-t)}}{b}\right) - \rho\eta(t)\sigma(t)\left(\frac{1-e^{-a(T-t)}}{a}\right)\right]dt + \eta(t)dW_2^T(t)$$

*where $W^T(t) = (W_1^T(t), W_2^T(t))'$ is a 2-dimensional $\mathbb{Q}^{\mathbb{T}}$ Brownian motion with instantaneous correlation equal to $\rho$.*

*Proof.* See Appendix A.3. □

**Proposition 6.** *The solution of $x(t)$ and $y(t)$ are, conditional on $\mathcal{F}_s$, given by*

$$x(t) = e^{-a(t-s)}x(s) - M_x^T(s,t) + \int_s^t \sigma(u)e^{-a(t-u)}dW_1^T(u)$$

$$y(t) = e^{-b(t-s)}y(s) - M_y^T(s,t) + \int_s^t \eta(u)e^{-b(t-u)}dW_2^T(u)$$

[7]See [3], Section 4.2.4 .



Electronic copy available at: https://ssrn.com/abstract=3598285

*where*

$$M_x^T(s,t) = \sum_{i=i(s)}^{i(t)} \left[ \left( \frac{\sigma_{i-1}^2}{a^2} + \rho \frac{\eta_{i-1}\sigma_{i-1}}{ab} \right) \left( e^{-a\Delta t_i^{(r)}} - e^{-a\Delta t_i^{(l)}} \right) \right.$$
$$- \frac{\sigma_{i-1}^2}{2a^2} \left( e^{-a\left(\Delta t_i^{(r)} + \Delta T_i^{(r)}\right)} - e^{-a\left(\Delta t_i^{(l)} + \Delta T_i^{(l)}\right)} \right)$$
$$\left. - \frac{\rho\eta_{i-1}\sigma_{i-1}}{b(a+b)} \left( e^{-a\Delta t_i^{(r)} - b\Delta T_i^{(r)}} - e^{-a\Delta t_i^{(l)} - b\Delta T_i^{(l)}} \right) \right]$$

*and*

$$M_y^T(s,t) = \sum_{i=i(s)}^{i(t)} \left[ \left( \frac{\eta_{i-1}^2}{b^2} + \rho \frac{\eta_{i-1}\sigma_{i-1}}{ab} \right) \left( e^{-b\Delta t_i^{(r)}} - e^{-b\Delta t_i^{(l)}} \right) \right.$$
$$- \frac{\eta_{i-1}^2}{2b^2} \left( e^{-b\left(\Delta t_i^{(r)} + \Delta T_i^{(r)}\right)} - e^{-b\left(\Delta t_i^{(l)} + \Delta T_i^{(l)}\right)} \right)$$
$$\left. - \frac{\rho\eta_{i-1}\sigma_{i-1}}{a(a+b)} \left( e^{-b\Delta t_i^{(r)} - a\Delta T_i^{(r)}} - e^{-b\Delta t_i^{(l)} - a\Delta T_i^{(l)}} \right) \right]$$

*where* $\Delta t_i^{(l)}$ *and* $\Delta t_i^{(r)}$ *are as in Proposition 2 and*

$$\Delta T_i^{(l)} = T - \max(s, t_{i-1}), \qquad \Delta T_i^{(r)} = T - \min(t, t_i)$$

*Proof.* See Appendix A.4. □

## 2.4 Pricing formulas

**Theorem 2.** *The price at time* $t$ *of a caplet that pays at time* $T_2$ *the amount*

$$N\alpha(T_1,T_2)\left[L(T_1,T_2) - X\right]^+$$

*is given by*

$$\mathbf{Cpl}(t,T_1,T_2,N,X) = P(t,T_1)N\Phi\left( \frac{\ln\frac{NP(t,T_1)}{N'P(t,2)}}{\Sigma(t,T_1,T_2)} - \frac{1}{2}\Sigma(t,T_1,T_2) \right)$$
$$- N(1+X\alpha(T_1,T_2))P(t,T_2)\Phi\left( \frac{\ln\frac{NP(t,T_1)}{N'P(t,2)}}{\Sigma(t,T_1,T_2)} - \frac{1}{2}\Sigma(t,T_1,T_2) \right)$$



Electronic copy available at: https://ssrn.com/abstract=3598285

*where the reset date $T_1$ satisfies $t < T_1 < T_2$, $L(T_1, T_2)$ is the floating rate between $T_1$ and $T_2$, fixed at $T_1$ and payed at $T_2$, $N$ is the nominal value, $\alpha(T_1, T_2)$ the year fraction between $T_1$ and $T_2$, and finally*

$$\begin{aligned}\Sigma(t,T,S) = \sum_{i=i(t)}^{i(T)} \Bigg\{ & \frac{\sigma_{i-1}^2}{2a^3}\left(1-e^{-a(S-T)}\right)^2\left[e^{-2a(T-\min(T,t_i))}-e^{-2a(T-\max(S,t_{i-1}))}\right] \\ & +\frac{\eta_{i-1}^2}{2b^3}\left(1-e^{-b(S-T)}\right)^2\left[e^{-2b(T-\min(T,t_i))}-e^{-2b(T-\max(S,t_{i-1}))}\right] \\ & +2\rho\frac{\sigma_{i-1}\eta_{i-1}}{ab(a+b)}\left(1-e^{-a(S-T)}\right)\left(1-e^{-b(S-T)}\right)\left[e^{-(a+b)(T-\min(T,t_i))}-e^{-(a+b)(T-\max(S,t_{i-1}))}\right]\Bigg\}\end{aligned}$$

*Proof.* The proof can be recovered from Chapter 4 of [3]. The only thing that needs to be changed in the p.c. specification is the variance of the logarithm of the zero-coupon bond price. Recalling Theorem 1, the forward measure variance of the logarithm of the price at time $T$ of the zero-coupon bond maturing in $S$, conditional on $\mathcal{F}_t$, is given by

$$\begin{aligned}V_p^2 &= \mathbb{V}^T\left[-\frac{1-e^{-a(S-T)}}{a}x(T)-\frac{1-e^{-b(S-T)}}{b}y(T)|\mathcal{F}_t\right] \\ &= \left(\frac{1-e^{-a(S-T)}}{a}\right)^2\mathbb{V}^T\left[x(T)|\mathcal{F}_t\right]+\left(\frac{1-e^{-b(S-T)}}{b}\right)^2\mathbb{V}^T\left[y(T)|\mathcal{F}_t\right] \\ &\quad +2\left(\frac{1-e^{-a(S-T)}}{a}\right)\left(\frac{1-e^{-b(S-T)}}{b}\right)\mathrm{Cov}^T\left[x(T),y(T)|\mathcal{F}_t\right]\end{aligned}$$

The variance of $x(T)$ is given by

$$\begin{aligned}\mathbb{V}^T\left[x(T)|\mathcal{F}_t\right] &= \mathbb{E}^T\left[\left(\int_t^T \sigma(u)e^{-a(T-u)}\,dW_1^T(u)\right)^2\right] \\ &= \int_t^T \sigma(u)^2 e^{-2a(T-u)}\,du \\ &= \sum_{i=i(t)}^{i(T)}\frac{\sigma_{i-1}^2}{2a}\left[e^{-2a(t-\min(t,t_i))}-e^{-2a(t-\max(s,t_{i-1}))}\right]\end{aligned}$$



Electronic copy available at: https://ssrn.com/abstract=3598285

and the covariance term $\mathrm{Cov}^T\left[x(T), y(T)|\mathcal{F}_t\right]$ is given by

$$\begin{aligned}\mathbb{E}^T\left[\left(\int_t^T \sigma(u)e^{-a(T-u)}\, dW_1^T(u)\right)\left(\int_t^T \eta(u)e^{-b(T-u)}\, dW_2^T(u)\right)\right] \\ = \int_t^T \rho\sigma(u)\eta(u)e^{-(a+b)(T-u)}\, du \\ = \sum_{i=i(s)}^{i(t)} \rho\frac{\sigma_{i-1}\eta_{i-1}}{(a+b)}\left[e^{-(a+b)(t-\min(t,t_i))} - e^{-(a+b)(t-\max(s,t_{i-1}))}\right]\end{aligned}$$

The calculations for $\mathbb{V}^T\left[y(T)|\mathcal{F}_t\right]$ are analogous to those for $\mathbb{V}^T\left[x(T)|\mathcal{F}_t\right]$. □

The price of a cap is simply given by the sum of the caplet prices.

**Corollary 2** (Cap price)**.** *The price at time $t$ of a cap composed by the caplets that pays at payment dates $\{T_1, \ldots, T_n\}$, with associated reset dates $\{T_0, \ldots, T_{n-1}\}$, strike $X$ and nominal value $N$ is given by*

$$\mathbf{Cap}(t, \mathcal{T}, N, X) = \sum_{i=1}^{n} \mathbf{Cpl}(t, T_{i-1}, T_i, N, X)$$

*where $\mathcal{T} = \{T_0, \ldots, T_n\}$.*

For what concerns the pricing of European swaptions, the pricing formula is the one given in Theorem 4.2.3 in [3], with the following changes:

- the terms $\mu_x$ and $\mu_y$ use the $M_x^T$ and $M_y^T$ given in Proposition 6;
- $\sigma_x$, $\sigma_y$ and $\rho_{xy}$ are the standard deviations and correlation coefficient of the processes $x$ and $y$ under the forward probability measure (which are equal to the ones under the risk-neutral measure). Recalling Proposition 1 and 6, we have that

$$\sigma_x^2 = \sum_{i=i(0)}^{i(T)} \frac{\sigma_{i-1}^2}{2a}\left(e^{-2a(T-\min(t,t_i))} - e^{-2a(T-\max(0,t_{i-1}))}\right)$$

$$\sigma_y^2 = \sum_{i=i(0)}^{i(T)} \frac{\eta_{i-1}^2}{2b}\left(e^{-2b(T-\min(t,t_i))} - e^{-2b(T-\max(0,t_{i-1}))}\right)$$

$$\rho_{xy} = \sum_{i=i(0)}^{i(T)} \frac{2\rho\sigma_{i-1}\eta_{i-1}}{a+b}\left(e^{-(a+b)(t-\min(t,t_i))} - e^{-(a+b)(t-\max(s,t_{i-1}))}\right)$$



Electronic copy available at: https://ssrn.com/abstract=3598285

- the $A$ function is given by

$$A(s,t) = \frac{P(0,t)}{P(0,s)} \exp\left\{\frac{1}{2}\left[V(s,t) - V(0,t) + V(0,s)\right]\right\}$$

where the $V$ function is the one introduced in Proposition 3.

# 3 Calibration

In this section we describe the procedure adopted for the calibration of the XG2++ model. In particular we will consider the calibration on a set of at-the-money (ATM) swaptions prices with maturities ranging from 1 year to 30 years, and tenors (the maturity of the underlying interest rate swaps) ranging from 1 to 30 years. Eventually, we will provide a description of the interpolation algorithm we have used for the piecewise-constant volatilities, that can be used to speed up the calculations.

## 3.1 Swaption calibration

Given a set of ATM swaptions and a term structure of interest rates, the model can be calibrated in order to fit the swaption prices as best as possible.

As input, we expect to have a swap curve and a set of swaption prices (or volatilities from which prices can be recovered) corresponding to different option expiries and swap tenors. More precisely, the input is a swaption price matrix $(s_{ij})$, where $i = 1, \dots, n$ represents the available maturities and $j = 1, \dots, m$ the available tenors. The swaption expiries are given by the times $t_1 < \cdots < t_n$, whereas the swap tenors are given by $\tau_1 < \cdots < \tau_m$.

We have used EUR data at the 2nd January, 2018. Market data are represented in Figure 3. The swaption volatilities are normal.

The main problem in the calibration to swaption data is that a usual swaption volatility surface can contain more than 200 swaption quotes. These can be associated with more than 20 different expiries, therefore each factor can have more than 20 different volatilities. This determines a numeric problem with a high dimensionality, which can be hard to solve. In addition, the choice of the optimization starting points is another matter of discussion. Our data contains 224 swaptions, corresponding to 16 expiries (1Yr, 18Mo, 2Yr, 3Yr, 4Yr, 5Yr, 6Yr, 7Yr, 8Yr, 9Yr, 10Yr, 12Yr, 15Yr, 20Yr, 25Yr, 30Yr) and 14 tenors (1Yr, 2Yr, 3Yr, 4Yr, 5Yr, 6Yr, 7Yr, 8Yr, 9Yr, 10Yr, 15Yr, 20Yr, 25Yr, 30Yr).

Our approach to the calibration is divided in different steps, which are described in detail in the following sections.



Electronic copy available at: https://ssrn.com/abstract=3598285

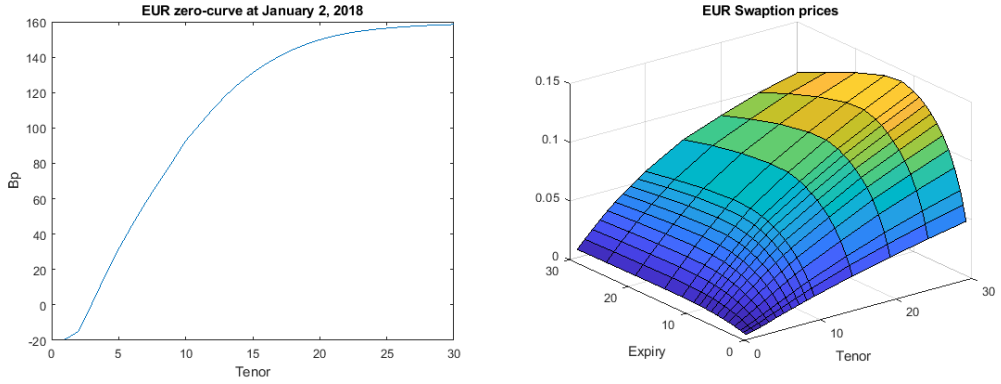


Figure 3: EUR bootstrapped zero-rate curve (left) and EUR swaption ATM prices (right) at January 2, 2018.

## 3.2 Step 1: Global constant G1++ calibration

The first step is to calibrate a G1++ model with constant parameters to the whole swaption volatility surface. We recall that a G1++ model can be specified as

$$dx(t) = -ax(t)dt + \sigma(t)dW(t), \quad x(0) = x_0$$

In the optimization, we use as initial point 0.05 for the mean-reversion speed parameter[8] and 0.01 for the volatility. We minimize the sum of squared differences between market and model swaption prices, using a nonlinear least-squares solver.

The goal of this step is to find a mean-reversion parameter that is a reasonable starting point for the following calibrations. The calibration fitting is represented in Figure 4.

## 3.3 Step 2: Bootstrapping piecewise-constant G1++ on swaption volatility surface slices

In this step, two piecewise-constant G1++ models are calibrated: The first is calibrated to the swaption volatility surface slice corresponding to the smallest swap tenor ($\tau = \tau_1$), whereas the second model is calibrated on the slice relative to the biggest tenor ($\tau = \tau_m$).

These calibrations are done in an incremental way, like in a bootstrapping procedure. More precisely, each G1++ model calibration consists of the following steps (we will consider the case $\tau = \tau_1$):

[8]This particular value can be found in some pricing software as a standard mean-reversion speed parameter.



Electronic copy available at: https://ssrn.com/abstract=3598285

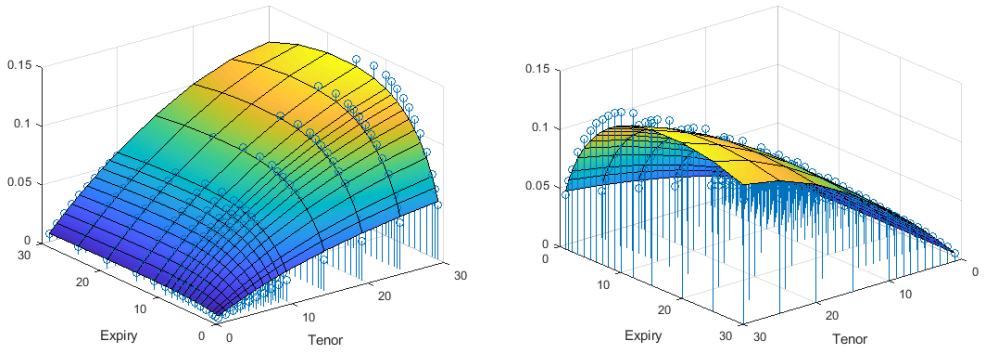


Figure 4: Step 1: G1++ model with constant parameters. The calibrated parameters are $a = 0.0309$ and $\sigma = 0.0078$. The model swaption prices are compared with market prices (dots).

- initialize a G1++ model with jump times corresponding to $t_1, \ldots, t_{n-1}$ (the option expiries, minus the last one), using as mean-reversion speed the parameter obtained from step 1;
- calibrate the first volatility $\sigma_0^s$ by optimizing with respect to the price of the first swaption price $s_{11}$;
- calibrate the second volatility $\sigma_1^s$ by optimizing with respect to the price of the first two swaption prices $s_{11}, s_{21}$ by keeping $\sigma_0^s$ constant (changing only $\sigma_1^s$);
- ...
- calibrate the last volatility $\sigma_{n-1}^s$ by optimizing with respect to the price of the all swaption prices $s_{11}, \ldots, s_{n1}$ by keeping $\sigma_0^s, \ldots, \sigma_{n-2}^s$ constant (changing only $\sigma_{n-1}^s$).

In this way, because we are calibrating $n$ volatilities over the same number of calibration instruments, we can perfectly recover the $n$ swaption prices. Moreover, the calibration is fast, since at each step only one volatility is calibrated. Calibrating on the other slice yields the volatilities $\eta_0^s, \ldots, \eta_n^s$.

Alternatively, this step could be performed using as calibration instruments caps, or floors. For example, the volatility structure relative to the first G1++ process can be derived from the ATM caps. Then, the second G1++ can be set equal to the first, or calibrated to Out-of-The-Money (OTM) caps. This variant of the second calibration step has the advantage to retain some information from both caps and swaptions.



Electronic copy available at: https://ssrn.com/abstract=3598285

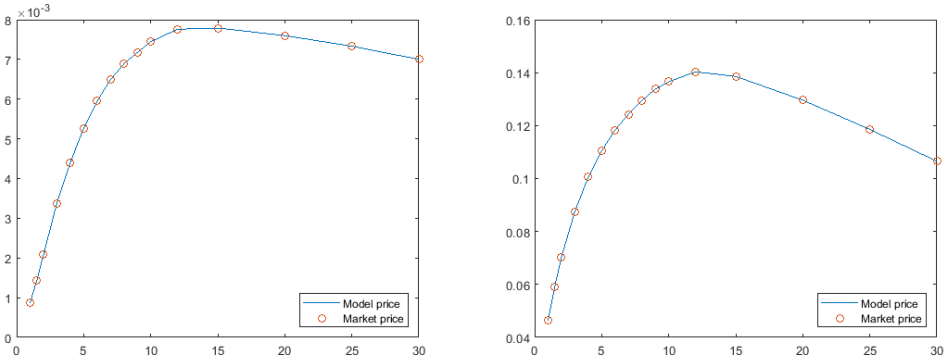


Figure 5: Step 2: piecewise-constant G1++ model calibrated to swaption surface slices corresponding to $\tau = 1$ (1 year, left) and $\tau = 30$ (30 years, right). The mean-reversion speed parameter is equal to 0.0309. The model swaption prices are compared with market prices (dots).

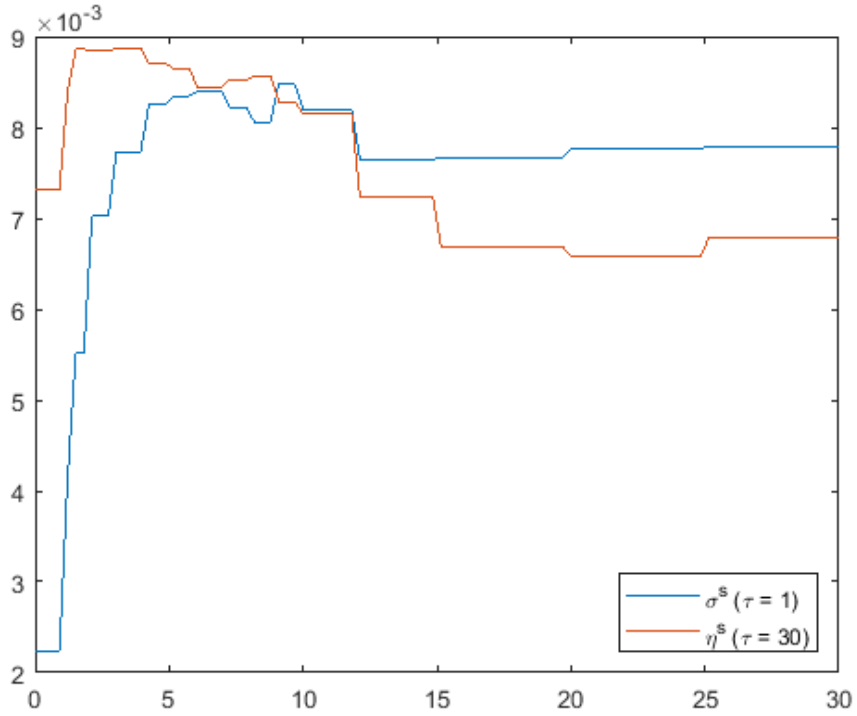


Figure 6: Step 2: piecewise-constant G1++ model calibrated to swaption surface slices corresponding to $\tau = 1$ (1 year, left) and $\tau = 30$ (30 years, right). Resulting piecewise-constant volatility structures. The mean-reversion speed parameter is equal to 0.0309.



Electronic copy available at: https://ssrn.com/abstract=3598285

## 3.4 Step 3: Global calibration

The last step is a global calibration on the whole swaption surface. The jump times are those introduced in Step 2. However, to reduce the dimensionality of the volatility parameters, we will assume that the volatility structures of the factors $x$ and $y$ of the XG2++ model are scalar multiplications of those obtained in Step 2. In other words, we assume that the volatility structure of the two factors is determined by the calibration on the two slices that has been performed in Step 2. More precisely, the vectors of the piecewise-constant volatilities that need to be calibrated $(\sigma_0, \ldots, \sigma_{n-1})$ and $(\eta_0, \ldots, \eta_{n-1})$ are given by

$$(\sigma_0, \ldots, \sigma_{n-1}) = \alpha(\sigma_0^s, \ldots, \sigma_{n-1}^s), \quad (\eta_0, \ldots, \eta_{n-1}) = \beta(\eta_0^s, \ldots, \eta_{n-1}^s)$$

where $\alpha, \beta \in \mathbb{R}^+$. Under these assumptions, the number of parameters reduce to 5: $a, b, \alpha, \beta, \rho$. The initial point of the calibration is given by the mean-reversion speed parameter obtained in Step 1 for both $a$ and $b$; $\alpha$ and $\beta$ are initialized to 1 and $\rho$ to 0. As in step 1, we minimize the sum of squared differences between market and model swaption prices.

## 3.5 Calibration results

The model fitting is shown in Figure 7, whereas the piecewise-constant final volatility structures are represented in Figure 8. Basically, the calibrated model is characterized by a persistent but low volatility (vector) component and a high but transitory one.

In addition, Table 1 summarizes the percentage differences errors of the swaption normal volatilities obtained with the calibration, whereas Table 2 contains the whole relative error data. Finally, Figure 9 shows the errors using a heatmap.

Considering that the highest relative errors are concentrated in the options with the shortest tenor (one year) and shortest maturity, we believe that these results show a reasonably good fit.

| | |
|---|---|
| Min | -10.5 % |
| Max | 60.8 % |
| Mean | 0.6 % |
| Mean abs | 5.3 % |

Table 1: Swaption volatility percentage differences (minimum error, maximum error, mean error and mean absolute error) for the EUR calibration. Number of swaptions: 224.



Electronic copy available at: https://ssrn.com/abstract=3598285

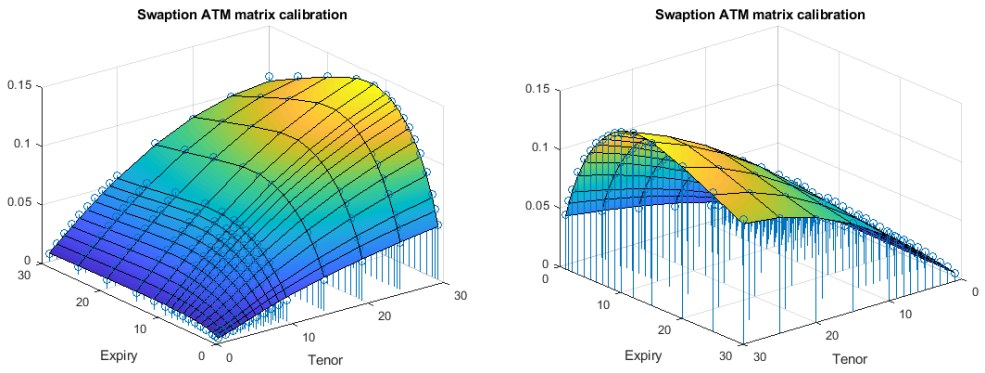


Figure 7: Step 3: The XG2++ model calibrated to the whole swaption surface (EUR). The model swaption prices are compared with market prices (dots). The mean-reversion speed parameters are $a = 0.9996, b = 0.0221$. The correlation parameter is $\rho = -0.9245$, whereas $\alpha = 6.3325$ and $\beta = 0.9544$.

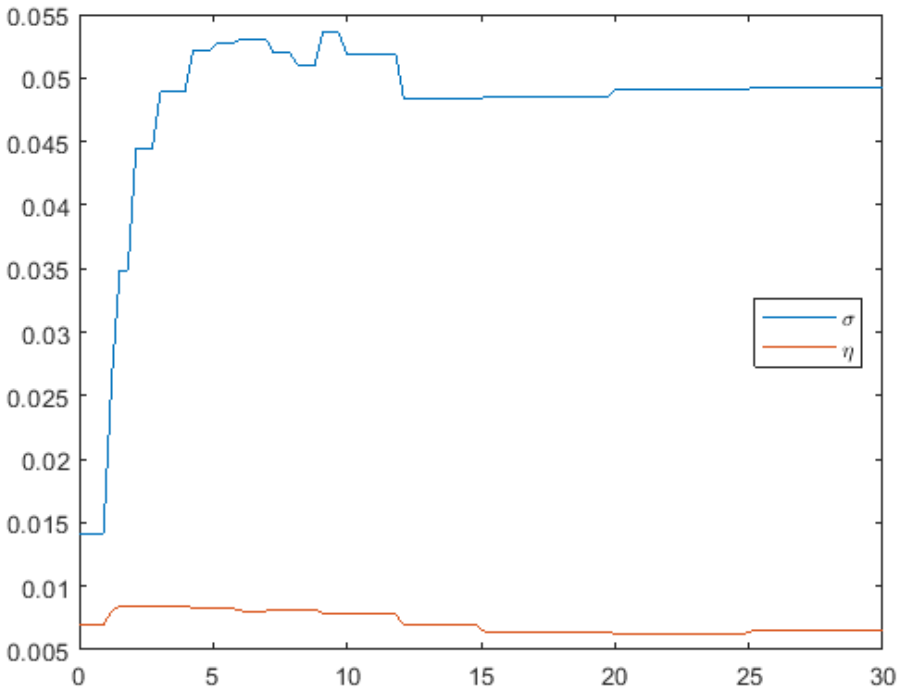


Figure 8: Step 3: XG2++ model volatility structures (EUR). The mean-reversion speed parameters are $a = 0.9996, b = 0.0221$. The correlation parameter is $\rho = -0.9249$, whereas $\alpha = 6.3325$ and $\beta = 0.9544$.



Electronic copy available at: https://ssrn.com/abstract=3598285

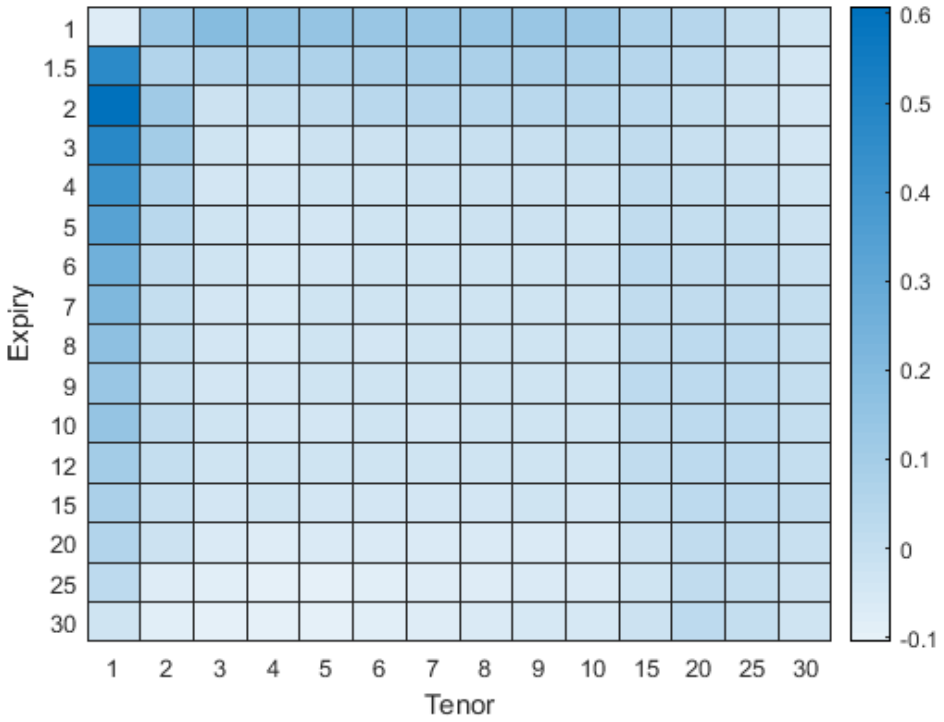


Figure 9: Swaption volatility percentage differences heatmap (EUR).



Electronic copy available at: https://ssrn.com/abstract=3598285

| | 1Yr | 2Yr | 3Yr | 4Yr | 5Yr | 6Yr | 7Yr | 8Yr | 9Yr | 10Yr | 15Yr | 20Yr | 25Yr | 30Yr |
|---|---|---|---|---|---|---|---|---|---|---|---|---|---|---|
| 1Yr | -7.8% | 12.2% | 19.5% | 15.4% | 14.2% | 13.5% | 13.3% | 14.0% | 13.3% | 12.3% | 7.3% | 4.4% | 0.4% | -2.8% |
| 18Mo | 46.5% | 5.8% | 5.5% | 6.9% | 6.6% | 7.3% | 9.4% | 8.4% | 7.8% | 6.6% | 4.5% | 1.9% | -1.2% | -3.9% |
| 2Yr | 60.8% | 11.0% | -1.9% | 0.5% | 0.9% | 3.7% | 4.6% | 3.8% | 3.4% | 3.0% | 2.8% | 0.0% | -2.3% | -4.0% |
| 3Yr | 47.6% | 9.8% | -3.2% | -4.9% | -2.7% | -2.5% | -1.4% | -0.6% | -0.6% | -0.3% | 1.0% | -0.6% | -1.9% | -4.0% |
| 4Yr | 41.0% | 5.2% | -4.9% | -4.2% | -3.6% | -3.2% | -1.9% | -1.9% | -1.8% | -1.7% | 1.5% | -0.1% | -1.0% | -3.0% |
| 5Yr | 33.6% | 4.0% | -2.7% | -4.5% | -4.2% | -3.3% | -2.9% | -2.7% | -2.6% | -2.8% | 1.1% | 0.2% | -0.3% | -2.0% |
| 6Yr | 26.0% | 1.4% | -3.7% | -5.1% | -3.9% | -3.0% | -3.0% | -2.8% | -2.9% | -2.7% | 2.0% | 1.2% | 0.9% | -1.2% |
| 7Yr | 21.4% | 0.1% | -3.9% | -5.0% | -3.4% | -3.3% | -3.0% | -3.0% | -3.3% | -3.2% | 1.6% | 1.4% | 1.5% | -0.2% |
| 8Yr | 16.3% | 0.5% | -4.5% | -5.2% | -3.8% | -4.0% | -3.7% | -3.8% | -3.3% | -2.9% | 1.7% | 2.1% | 1.9% | 0.2% |
| 9Yr | 13.0% | -0.5% | -4.6% | -4.8% | -3.5% | -3.5% | -3.5% | -3.4% | -3.2% | -3.0% | 2.0% | 2.5% | 2.2% | 0.5% |
| 10Yr | 14.5% | 0.7% | -3.8% | -4.7% | -3.9% | -3.8% | -3.8% | -3.7% | -3.2% | -3.4% | 1.2% | 2.1% | 2.3% | 0.6% |
| 12Yr | 10.5% | 0.0% | -3.7% | -3.4% | -3.6% | -3.6% | -3.7% | -3.5% | -3.1% | -3.4% | 1.0% | 2.4% | 2.3% | 0.6% |
| 15Yr | 8.1% | -0.6% | -3.8% | -3.7% | -4.4% | -4.5% | -4.0% | -4.1% | -3.6% | -4.2% | 0.4% | 2.3% | 2.0% | 0.7% |
| 20Yr | 5.5% | -2.4% | -6.1% | -7.2% | -7.0% | -7.0% | -6.6% | -6.5% | -6.6% | -6.6% | -2.0% | 1.0% | 0.9% | -0.6% |
| 25Yr | 2.8% | -7.3% | -8.8% | -9.6% | -9.9% | -8.6% | -8.0% | -7.4% | -7.1% | -6.8% | -2.8% | 0.9% | 0.2% | -2.1% |
| 30Yr | -3.6% | -8.7% | -9.6% | -10.4% | -10.5% | -8.9% | -7.8% | -6.5% | -5.6% | -5.5% | -1.7% | 1.8% | 0.1% | -3.8% |

Table 2: Swaption volatility percentage differences (EUR). Rows represent different expiries, whereas columns different maturities.



Electronic copy available at: https://ssrn.com/abstract=3598285

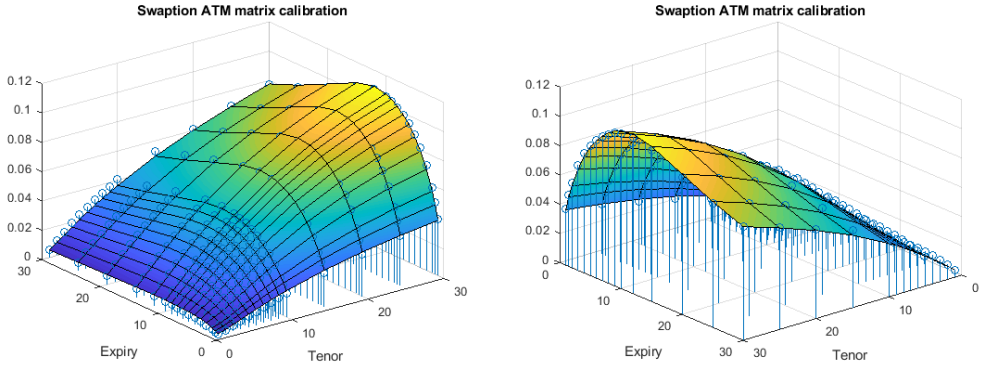


Figure 10: The XG2++ model calibrated to the whole USD swaption surface. The model swaption prices are compared with market prices (dots). The mean-reversion speed parameters are $a = 0.9829, b = 0.0181$. The correlation parameter is $\rho = -0.7463$.

## 3.6 Calibration on USD data

In order to verify the behaviour of the calibration procedure on different market data, we have performed the calibration on USD data. The model fitting is shown in Figure 10, whereas the piecewise-constant final volatility structures are represented in Figure 11. Table 3 summarizes the percentage differences errors of the swaption normal volatilities obtained with the calibration, whereas Table 4 contains the whole relative error data. Finally, Figure 12 shows the errors using a heatmap.

We believe that these results confirm the fitting capabilities of the model.

| | |
|---|---|
| Min | -10.3 % |
| Max | 23.3 % |
| Mean | -0.3 % |
| Mean abs | 3.2 % |

Table 3: Swaption volatility percentage differences (minimum error, maximum error, mean error and mean absolute error) for the USD calibration. Number of swaptions: 196.



Electronic copy available at: https://ssrn.com/abstract=3598285

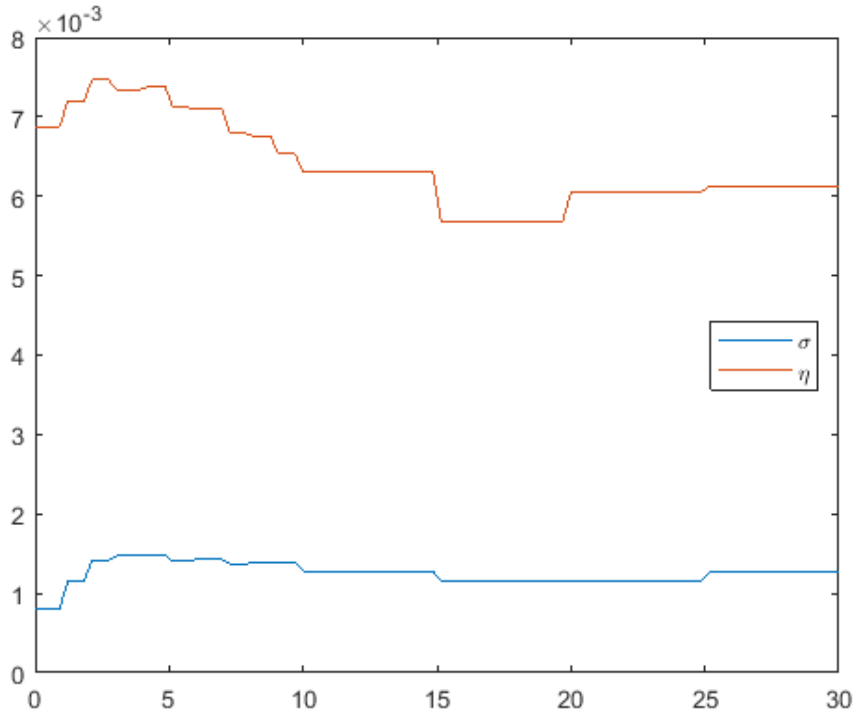


Figure 11: Step 3: XG2++ model volatility structures for the USD calibration. The mean-reversion speed parameters are $a = 0.9829, b = 0.0181$. The correlation parameter is $\rho = -0.7463$.



Electronic copy available at: https://ssrn.com/abstract=3598285

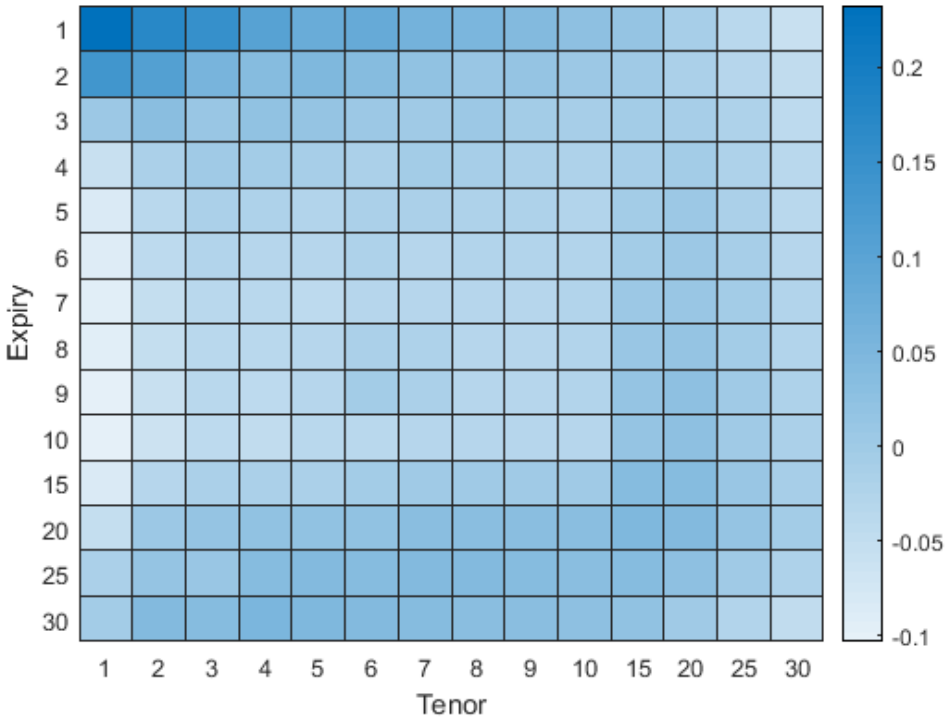


Figure 12: Swaption volatility percentage differences heatmap for the USD calibration.



Electronic copy available at: https://ssrn.com/abstract=3598285

Electronic copy available at: https://ssrn.com/abstract=3598285



| | 1Yr | 2Yr | 3Yr | 4Yr | 5Yr | 6Yr | 7Yr | 8Yr | 9Yr | 10Yr | 15Yr | 20Yr | 25Yr | 30Yr |
|---|---|---|---|---|---|---|---|---|---|---|---|---|---|---|
| 1Yr | 23.3% | 17.2% | 15.0% | 10.7% | 7.9% | 8.5% | 6.4% | 5.3% | 4.1% | 2.8% | 1.5% | -1.3% | -3.6% | -6.0% |
| 2Yr | 13.4% | 11.1% | 5.5% | 3.6% | 4.6% | 3.4% | 2.1% | 1.2% | 1.3% | 0.2% | -0.3% | -1.7% | -3.5% | -5.0% |
| 3Yr | 0.3% | 2.8% | 0.9% | 2.2% | 1.4% | 0.6% | 0.0% | 0.4% | -0.4% | -1.2% | -0.8% | -0.9% | -2.3% | -4.5% |
| 4Yr | -5.6% | -1.9% | 0.1% | -0.5% | -1.2% | -1.5% | -0.8% | -1.3% | -1.8% | -2.4% | -1.3% | -0.4% | -1.9% | -4.0% |
| 5Yr | -8.3% | -3.7% | -1.8% | -2.0% | -2.5% | -1.6% | -1.8% | -2.2% | -2.3% | -2.6% | -0.5% | 0.2% | -1.5% | -3.6% |
| 6Yr | -8.9% | -4.4% | -2.6% | -3.0% | -3.3% | -2.4% | -3.2% | -2.6% | -2.6% | -2.8% | -0.3% | 0.6% | -1.2% | -3.1% |
| 7Yr | -9.5% | -5.3% | -3.5% | -3.8% | -4.1% | -3.1% | -3.0% | -3.0% | -3.0% | -2.9% | 0.4% | 1.2% | -0.7% | -2.8% |
| 8Yr | -9.7% | -5.5% | -3.7% | -4.0% | -3.2% | -1.5% | -2.3% | -3.0% | -3.1% | -2.9% | 0.9% | 1.7% | -0.6% | -2.4% |
| 9Yr | -9.9% | -5.7% | -4.0% | -4.2% | -3.3% | -0.6% | -1.4% | -3.1% | -3.0% | -2.9% | 1.3% | 2.3% | -0.1% | -2.2% |
| 10Yr | -10.3% | -6.1% | -4.4% | -4.5% | -3.7% | -3.5% | -3.4% | -3.3% | -3.1% | -3.0% | 1.5% | 2.6% | 0.0% | -1.9% |
| 15Yr | -8.2% | -3.2% | -1.7% | -1.5% | -1.4% | -0.4% | -0.3% | 0.0% | 0.1% | 0.2% | 3.6% | 3.7% | 1.1% | -1.2% |
| 20Yr | -5.2% | 0.2% | 1.7% | 1.8% | 2.0% | 1.9% | 2.9% | 2.9% | 3.1% | 3.1% | 4.8% | 4.2% | 1.3% | -0.8% |
| 25Yr | -1.5% | 1.5% | 1.1% | 3.5% | 4.2% | 3.8% | 4.3% | 3.9% | 3.5% | 3.1% | 3.8% | 2.6% | -0.2% | -2.4% |
| 30Yr | -0.8% | 4.0% | 3.4% | 5.2% | 4.8% | 4.1% | 3.5% | 2.9% | 3.2% | 2.6% | 1.8% | -0.1% | -2.6% | -5.0% |

Table 4: Swaption volatility percentage differences for the USD calibration. Rows represent different expiries, whereas columns different maturities.

## 3.7 Robustness

An important topic when dealing with a model calibration is its robustness[9]. This is more important for models that are calibrated on historical data, where statistical significance of parameters is paramount; however, having a calibration procedure that produces similar parameters with similar input data is always desirable.

The robustness of the procedure we have outlined, mainly relies on the determination of the "global" G1++ mean-reversion parameter obtained in step 1. As described in Section 3.2, our choice of initial values for the G1++ parameters are 0.05 for the mean-reversion speed and 0.01 for the volatility. One can argue that this choice is completely arbitrary and nobody guarantees that starting from different values the final calibration result would be the same.

This is not the case. We have stressed the initial point, trying many different values, and the G1++ calibrated parameters that we obtain are remarkably stable ($\alpha = 3.09\%$ and $\sigma = 0.78\%$ for the EUR and $\alpha = 3.37\%$ and $\sigma = 0.82\%$ for the USD). Interestingly, the EUR and USD parameters are quite similar.

In order to test the ability of the model of consistently fitting market data, we have repeated the calibration at different dates, using data which greatly differ from the ones used so far. In Figure 13, the EUR zero curve and ATM swaption prices goodness-of-fit are shown. Notice that the zero curve is significantly different from the previous one, showing negative interest rates level across all tenors and a significant inversion at very high maturities. However, the fitting on swaption prices is still good, which is confirmed by the results reported in Table 5, which shows a worse (but acceptable) fitting for the May 2020 calibration on Euro.

In Figure 14 and Table 6 we report the same analysis for USD data, which, eventually, shows an even better goodness-of-fit overall.

## 3.8 Volatility interpolation

Depending on the procedure used in step 2, it may be the case that the swaption maturities of the swaptions don't match the jump times of the piecewise-constant volatility function[10]. In those cases an interpolation is necessary. Since the calibration instruments (the swaptions) can be in the

[9] See [2] for an in-depth discussion of some desirable characteristics of interest rate models.

[10] This is the case, for example, when caps, or floors, are used for bootstrapping the initial volatility (term) structure.



Electronic copy available at: https://ssrn.com/abstract=3598285

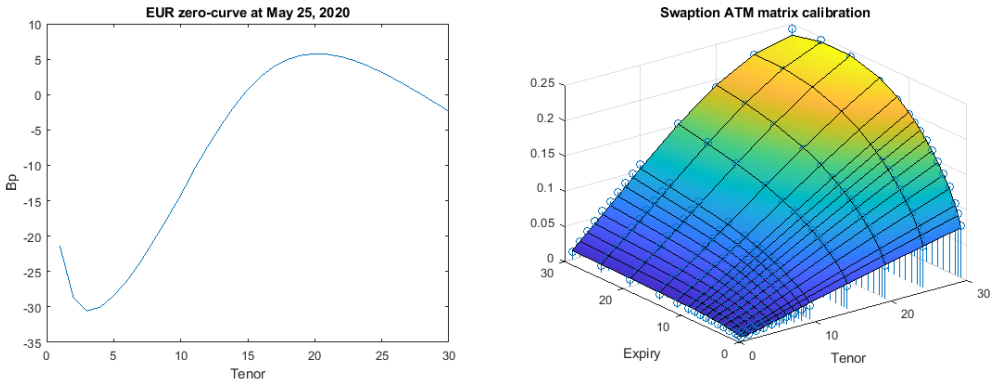


Figure 13: EUR bootstrapped zero-rate curve (left) and EUR swaption ATM prices (right). Both market and model prices are shown as of May 25, 2020. In this calibration we get the following parameters values: $a = 0.7340$, $b = 0.0103$ and $\rho = -0.9999$.

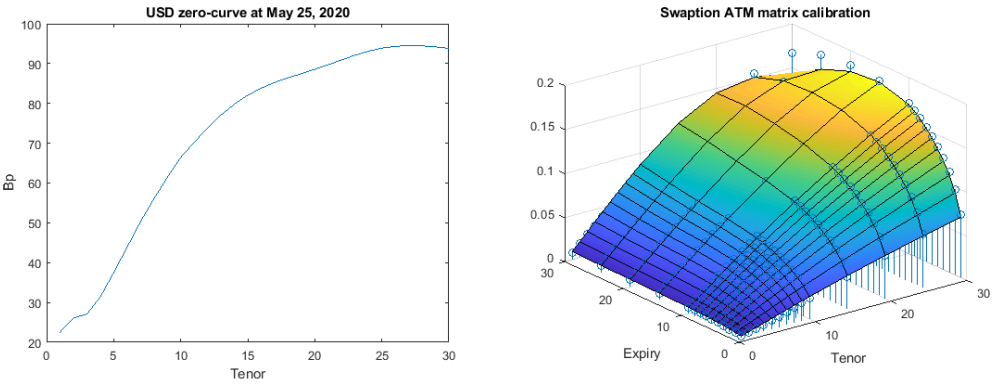


Figure 14: USD bootstrapped zero-rate curve (left) and USD swaption ATM prices (right). Both market and model prices are shown as of May 25, 2020. In this calibration we get the following parameters values: $a = 0.9998$, $b = 0.0048$ and $\rho = -0.8875$.



Electronic copy available at: https://ssrn.com/abstract=3598285

| | Jan 2018 | May 2020 |
|---|---|---|
| Min | -10.5 % | -23.1 % |
| Max | 60.8 % | 63.7 % |
| Mean | 0.6 % | 3.2 % |
| Mean abs | 5.3 % | 6.8 % |
| Min | -5.4 | -6.0 |
| Max | 23.4 | 28.3 |
| Mean | 0.1 | 1.4 |
| Mean abs | 2.8 | 3.2 |

Table 5: Swaption volatility percentage differences (minimum error, maximum error, mean error and mean absolute error) for the EUR calibration at different dates (upper half of the table) and swaption volatility differences (lower half of the table, in basis points). Number of swaptions: 224.

| | Jan 2018 | May 2020 |
|---|---|---|
| Min | -10.3 % | -14.5 % |
| Max | 23.3 % | 28.4 % |
| Mean | -0.3 % | 0.1 % |
| Mean abs | 3.2 % | 4.9 % |
| Min | -6.9 | -7.2 |
| Max | 10.2 | 11.3 |
| Mean | -0.4 | -0.2 |
| Mean abs | 1.9 | 2.6 |

Table 6: Swaption volatility percentage differences (minimum error, maximum error, mean error and mean absolute error) for the USD calibration at different dates (upper half of the table) and swaption volatility differences (lower half of the table, in basis points). Number of swaptions: 196.

number of hundreds, it may be reasonable to improve the speed of the interpolation algorithm. Generally, interpolation algorithms search the known data points in order to find the interval where the point that has to be interpolated falls. Binary search and interpolation search can accomplish this task very efficiently (see [12]), but often require that the searched key possess some characteristics. For example, interpolation search requires that keys are distributed uniformly[11].

Unfortunately, in our case the maturities, or tenors, which are the keys that have to be searched, are distributed arbitrarily on the (positive) real

[11] Actually, this requirement can be generalized since a known distribution function can be mapped to a uniform distribution.



Electronic copy available at: https://ssrn.com/abstract=3598285

axis. When this task has to be repeated several times, it may be clever to do a first interpolation where new (interpolated) data are added to the known ones, so that the set of initial points is "better" spaced. First, observe that all the tenors are a multiple of some year fraction (a semester, a quarter, or a month). Therefore, the time range of available maturities can be subdivided in equally spaced sub-intervals relative to the smallest common year fraction, so that their endpoints are either both within observed maturities, or one, or both of them match observed maturities. Second, we can interpolate on those new points and store the corresponding volatility values. Finally, interpolations can be performed as follows[12]:

- find the time interval where the unknown value with maturity $t$ belongs. This is equal to $\left[t_{m(t)}, t_{m(t)+1}\right)$, where $m(t) = \lfloor t\delta^{-1} \rfloor$, $\delta$ is the smallest common year fraction and $\lfloor x \rfloor$ is a function that rounds $x$ to the smallest integer;
- if $m(t) > n$, where $n$ is the total number of intervals, then $\sigma(t) = \sigma_n$ else $\sigma(t) = \sigma_{m(t)}$.

Notice that once the equally spaced interpolated values are stored, the only tasks that need to be performed again are the ones indicated with bullet points.

For example, suppose we have known information on volatility at times equal to 6 months, 1 year and a half, and 5 year and a half. We can subdivide the time range in intervals of identical length, say 6 months, so that we end up with 12 points delimiting 11 time intervals. Now, suppose we want to know the value of volatility at time 2.2 years: you simply multiply 2.2 by 2 (the reciprocal of 0.5, or six months) and take the integer part of the resulting number, which is 4. That is, the unknown volatility value belongs to the fifth interval which is, obviously, between 2 and 2.5 years. Although this example may seem trivial, when the number of interpolations that have to be performed is very high, it can save a considerable amount of time because it requires only a simple multiplication instead of a number of comparisons.

## 3.9 A technical remark

Since the calibration procedure perfectly fits the swaption volatility surface slices, the model can be considered to be "no-arbitrage" with respect to the

[12]What we have considered here is the interpolation of a the piecewise-continuos volatility function. The same algorithm can be applied to other quantities, such as interest rates, which can be approximated by means of other approximating functions, e.g. linear interpolation.



Electronic copy available at: https://ssrn.com/abstract=3598285

instruments corresponding to those slices. Something similar is done when a piecewise-constant G1++ model is utilized to price bermudan swaptions, for example when dealing with callable bonds. However, in our calibration we are not dropping any calibration instrument, but we are assuming that the information about the whole volatility surface can be expressed in terms of the information recovered from the two slices that we have considered. This is a big simplification, which reduces the surface shapes that the model can generate. However, the dimensionality reduction is dramatic and this helps us quickly calibrate the model on over 200 calibration instruments, reducing specification issues.

# 4 Conclusions

In this paper we have described a procedure which provides a fast and reliable way to calibrate a G2++ model with piecewise-constant volatility. Although this model retain the simple dynamics of the G2++, it can fit interest rate option prices much better than the standard version of G2++ since it can convey more information on the term structure of the implied volatility. Moreover, the algorithm is easy to implement and to maintain because it doesn't require a particular ability to be tuned. The only choice that a user is required to make is the selection of the derivatives (caps or swaptions) on which she wants to initialise the volatility structures. In addition, one could argue that the piecewise-constant formulation of the volatility is arbitrary and other deterministic functions could be used to produce different volatility structures. However, we believe that, if there are no particular reasons to choose a specific volatility functional form, the piecewise-constant formulation is a good choice, because it is very general and flexible. A limitation of the model is it doesn't capture the "smile" on OTM options. Mixing two or more processes should overcome this limitation and this could be the subject for future research. Nevertheless, we think the model can have interesting applications especially in Monte Carlo simulations where many risk factors, other than interest rate, are simultaneously combined.



Electronic copy available at: https://ssrn.com/abstract=3598285

# A Proofs

## A.1 The short rate distribution (proposition 2)

*Proof.* Since the short rate is the sum of deterministic functions and stochastic integrals, it is normal. The expected value is obvious from Proposition 1. For the variance,

$$\mathbb{V}\left[r(t)|\mathcal{F}_s\right] =$$

$$\mathbb{E}\left\{\left[\sum_{i=i(s)}^{i(t)}\left(\sigma_{i-1}\int_{\max(s,t_{i-1})}^{\min(t,t_i)}e^{-a(t-u)}dW_1(u)+\eta_{i-1}\int_{\max(s,t_{i-1})}^{\min(t,t_i)}e^{-b(t-u)}dW_2(u)\right)\right]^2|\mathcal{F}_s\right\}$$

$$=\mathbb{E}\left[\left(\sum_{i=i(s)}^{i(t)}\sigma_{i-1}\int_{\max(s,t_{i-1})}^{\min(t,t_i)}e^{-a(t-u)}dW_1(u)\right)^2+\left(\sum_{i=i(s)}^{i(t)}\eta_{i-1}\int_{\max(s,t_{i-1})}^{\min(t,t_i)}e^{-b(t-u)}dW_2(u)\right)^2\right.$$

$$\left.+2\left(\sum_{i=i(s)}^{i(t)}\sigma_{i-1}\int_{\max(s,t_{i-1})}^{\min(t,t_i)}e^{-a(t-u)}dW_1(u)\right)\left(\sum_{i=i(s)}^{i(t)}\eta_{i-1}\int_{\max(s,t_{i-1})}^{\min(t,t_i)}e^{-b(t-u)}dW_2(u)\right)|\mathcal{F}_s\right]$$

Now, for $i\neq j$, the integration intervals

$$[\max(s,t_{i-1}),\min(t,t_i)]\quad[\max(s,t_{j-1}),\min(t,t_j)]$$

are disjoint, therefore all integrals products like

$$\mathbb{E}\left[\left(\int_{\max(s,t_{i-1})}^{\min(t,t_i)}e^{-a(t-u)}dW_1(u)\right)\left(\int_{\max(s,t_{j-1})}^{\min(t,t_j)}e^{-a(t-u)}dW_1(u)\right)|\mathcal{F}_s\right]$$

are equal to zero. So,

$$\mathbb{V}\left[r(t)|\mathcal{F}_s\right]=\sum_{i=i(s)}^{i(t)}\sigma_{i-1}^2\int_{\max(s,t_{i-1})}^{\min(t,t_i)}e^{-2a(t-u)}du+\sum_{i=i(s)}^{i(t)}\eta_{i-1}^2\int_{\max(s,t_{i-1})}^{\min(t,t_i)}e^{-2b(t-u)}du$$

$$+2\rho\sum_{i=i(s)}^{i(t)}\sigma_{i-1}\eta_{i-1}\int_{\max(s,t_{i-1})}^{\min(t,t_i)}e^{-(a+b)(t-u)}du=\sum_{i=i(s)}^{i(t)}\left[\frac{\sigma_{i-1}^2}{2a}\left(e^{-2a\Delta t_i^{(r)}}-e^{-2a\Delta t_i^{(l)}}\right)\right.$$

$$\left.+\sum_{i=i(s)}^{i(t)}\frac{\eta_{i-1}^2}{2b}\left(e^{-2b\Delta t_i^{(r)}}-e^{-2b\Delta t_i^{(l)}}\right)+\sum_{i=i(s)}^{i(t)}\frac{2\rho\sigma_{i-1}\eta_{i-1}}{a+b}\left(e^{-(a+b)\Delta t_i^{(r)}}-e^{-(a+b)\Delta t_i^{(l)}}\right)\right]$$

□



Electronic copy available at: https://ssrn.com/abstract=3598285

## A.2 The integrated process (proposition 3)

*Proof.* The integrated process is given by

$$\int_s^t r(u)du = \int_s^t \varphi(u)du + x(s)\int_s^t e^{-a(u-s)}du + y(s)\int_s^t e^{-a(u-s)}du + \int_s^t \int_s^\xi \sigma(u)e^{-a(\xi-u)}dW_1(u)\ d\xi + \int_s^t \int_s^\xi \eta(u)e^{-b(\xi-u)}dW_2(u)\ d\xi$$

So, since it is a sum of deterministic functions and stochastic integrals, it is normal. Moreover, since the stochastic integrals have zero mean,

$$\mathbb{E}\left[I(s,t)|\mathcal{F}_s\right] = \int_s^t \varphi(u)du + x(s)\int_s^t e^{-a(u-s)}du + y(s)\int_s^t e^{-a(u-s)}du = \int_s^t \varphi(u)du + x(s)\frac{1-e^{-a(t-s)}}{a} + y(s)\frac{1-e^{-b(t-s)}}{b}$$

Changing the order of integration of the stochastic integral yields

$$\int_s^t \int_s^\xi \sigma(u)e^{-a(\xi-u)}dW_1(u)\ d\xi = \int_s^t \int_u^t \sigma(u)e^{-a(\xi-u)}d\xi\ dW_1(u) = \int_s^t \sigma(u)\int_u^t e^{-a(\xi-u)}d\xi\ dW_1(u) = \int_s^t \sigma(u)\left(\frac{1-e^{-a(t-u)}}{a}\right)\ dW_1(u)$$

So, the random variable

$$\int_s^t \int_s^\xi \sigma(u)e^{-a(\xi-u)}dW_1(u)\ d\xi$$

is normal with zero mean and variance given by

$$\mathbb{E}\left[\left(\int_s^t \sigma(u)\left(\frac{1-e^{-a(t-u)}}{a}\right)\ dW_1(u)\right)^2\right] = \int_s^t \left[\sigma(u)\left(\frac{1-e^{-a(t-u)}}{a}\right)\right]^2\ du = \sum_{i=i(s)}^{i(t)} \frac{\sigma_{i-1}^2}{a^2}\int_{\max(s,t_{i-1})}^{\min(t,t_i)} \left(1-e^{-a(t-u)}\right)^2\ du$$

Now,

$$\int_{\max(s,t_{i-1})}^{\min(t,t_i)} \left(1-e^{-a(t-u)}\right)^2\ du = \int_{\max(s,t_{i-1})}^{\min(t,t_i)} \left(1-2e^{-a(t-u)}+e^{-2a(t-u)}\right)\ du = \left(\Delta t_i^{(l)} - \Delta t_i^{(r)}\right) - \frac{2}{a}\left(e^{-a\Delta t_i^{(r)}} - e^{-a\Delta t_i^{(l)}}\right) + \frac{1}{2a}\left(e^{-2a\Delta t_i^{(r)}} - e^{-2a\Delta t_i^{(l)}}\right)$$



Electronic copy available at: https://ssrn.com/abstract=3598285

So, we have

$$\sum_{i=i(s)}^{i(t)} \frac{\sigma_{i-1}^2}{a^2} \int_{\max(s,t_{i-1})}^{\min(t,t_i)} \left(1 - e^{-a(t-u)}\right)^2 \, du =$$

$$\sum_{i=i(s)}^{i(t)} \frac{\sigma_{i-1}^2}{a^2} \left[ \left(\Delta t_i^{(l)} - \Delta t_i^{(r)}\right) - \frac{2}{a}\left(e^{-a\Delta t_i^{(r)}} - e^{-a\Delta t_i^{(l)}}\right) + \frac{1}{2a}\left(e^{-2a\Delta t_i^{(r)}} - e^{-2a\Delta t_i^{(l)}}\right) \right]$$

The variance of the second integral is calculated analogously. Finally, we need to calculate the covariance between the integrals

$$\int_s^t \int_s^\xi \sigma(u) e^{-a(\xi-u)} dW_1(u) \, d\xi \quad \int_s^t \int_s^\xi \eta(u) e^{-n(\xi-u)} dW_2(u) \, d\xi$$

By Ito's isometry,

$$\mathbb{E}\left[\int_s^t \int_s^\xi \sigma(u) e^{-a(\xi-u)} dW_1(u) \, d\xi \int_s^t \int_s^\xi \eta(u) e^{-n(\xi-u)} dW_2(u) \, d\xi\right] =$$

$$\mathbb{E}\left[\int_s^t \sigma(u) \left(\frac{1 - e^{-a(t-u)}}{a}\right) dW_1(u) \int_s^t \eta(u) \left(\frac{1 - e^{-b(t-u)}}{b}\right) dW_2(u)\right] =$$

$$\int_s^t \rho\sigma(u)\eta(u) \left(\frac{1 - e^{-a(t-u)}}{a}\right)\left(\frac{1 - e^{-b(t-u)}}{b}\right) du =$$

$$\sum_{i=i(s)}^{i(t)} \frac{\rho\sigma_{i-1}\eta_{i-1}}{ab} \int_{\max(s,t_{i-1})}^{\min(t,t_i)} \left(1 - e^{-a(t-u)} - e^{-b(t-u)} + e^{-(a+b)(t-u)}\right) du =$$

$$\sum_{i=i(s)}^{i(t)} \frac{\rho\sigma_{i-1}\eta_{i-1}}{ab} \left[ \left(\Delta t_i^{(l)} - \Delta t_i^{(r)}\right) - \frac{1}{a}\left(e^{-a\Delta t_i^{(r)}} - e^{-a\Delta t_i^{(l)}}\right) \right.$$

$$\left. - \frac{1}{b}\left(e^{-b\Delta t_i^{(r)}} - e^{-b\Delta t_i^{(l)}}\right) + \frac{1}{a+b}\left(e^{-(a+b)\Delta t_i^{(r)}} - e^{-(a+b)\Delta t_i^{(l)}}\right) \right]$$

□

## A.3 The forward measure (proposition 5)

*Proof.* Let's start by noticing that the integral process

$$\int_0^T [x(u) + y(u)] \, du = \int_0^T \sigma(u) \left(\frac{1 - e^{-a(T-u)}}{a}\right) dW_1(u)$$

$$+ \int_0^T \eta(u) \left(\frac{1 - e^{-b(T-u)}}{b}\right) dW_2(u)$$



Electronic copy available at: https://ssrn.com/abstract=3598285

can be written equivalently by means of a two-dimensional standard $\mathbb{Q}$ Brownian motion $\widetilde{W}(t)$ in the following way,

$$\int_0^T [x(u)+y(u)]\ du = \int_0^T \sigma(u)\left(\frac{1-e^{-a(T-u)}}{a}\right)\ d\widetilde{W}_1(u)$$
$$+\int_0^T \rho\eta(u)\left(\frac{1-e^{-b(T-u)}}{b}\right)\ d\widetilde{W}_1(u)+\int_0^T \sqrt{1-\rho^2}\,\eta(u)\left(\frac{1-e^{-b(T-u)}}{b}\right)\ d\widetilde{W}_2(u)$$
$$= \int_0^T \begin{bmatrix} \sigma(u)\left(\frac{1-e^{-a(T-u)}}{a}\right)+\rho\eta(u)\left(\frac{1-e^{-b(T-u)}}{b}\right) \\ \sqrt{1-\rho^2}\,\eta(u)\left(\frac{1-e^{-b(T-u)}}{b}\right) \end{bmatrix} \cdot \begin{bmatrix} d\widetilde{W}_1(u) \\ d\widetilde{W}_2(u) \end{bmatrix}$$

where we have used the fact that the bidimensional correlated Brownian motion $W$ can be represented as

$$\begin{bmatrix} W_1(u) \\ W_2(u) \end{bmatrix} = \begin{bmatrix} 1 & 0 \\ \rho & \sqrt{1-\rho^2} \end{bmatrix} \begin{bmatrix} \widetilde{W}_1(u) \\ \widetilde{W}_2(u) \end{bmatrix}$$

Now, we introduce the process $\psi^T$ as

$$\psi^T(u) = -\begin{bmatrix} \sigma(u)\left(\frac{1-e^{-a(T-u)}}{a}\right)+\rho\eta(u)\left(\frac{1-e^{-b(T-u)}}{b}\right) \\ \sqrt{1-\rho^2}\,\eta(u)\left(\frac{1-e^{-b(T-u)}}{b}\right) \end{bmatrix}$$

Then,

$$\int_0^T \left\|\psi^T(u)\right\|^2\ du = \int_0^T \left\{ \left[\sigma(u)\left(\frac{1-e^{-a(T-u)}}{a}\right)+\rho\eta(u)\left(\frac{1-e^{-b(T-u)}}{b}\right)\right]^2 \right.$$
$$\left. + \left[\sqrt{1-\rho^2}\,\eta(u)\left(\frac{1-e^{-b(T-u)}}{b}\right)\right]^2 \right\}\ du$$
$$= \int_0^T \left[\sigma(u)^2\left(\frac{1-e^{-a(T-u)}}{a}\right)^2+\rho^2\eta(u)^2\left(\frac{1-e^{-b(T-u)}}{b}\right)^2 \right.$$
$$+ 2\rho\sigma(u)\eta(u)\left(\frac{1-e^{-a(T-u)}}{a}\right)\left(\frac{1-e^{-b(T-u)}}{b}\right)+$$
$$\left. + \left(1-\rho^2\right)\eta(u)^2\left(\frac{1-e^{-b(T-u)}}{b}\right)^2\right]\ du = V(0,T)$$



Electronic copy available at: https://ssrn.com/abstract=3598285

So, we have that

$$\begin{aligned}\frac{d\mathbb{Q}^T}{d\mathbb{Q}} &= \exp\left\{-\frac{1}{2}V(0,T) - \int_0^T \left[x(u)+y(u)\right]\ du\right\} \\ &= \exp\left\{\int_0^T \psi^T(u)\cdot d\widetilde{W}(u) - \frac{1}{2}\int_0^T \left\|\psi^T(u)\right\|^2\ du\right\}\end{aligned}$$

Therefore, $\psi^T$ satisfies the hypotheses of Theorem 11.3 in [1], so by Girsanov's Theorem the process

$$d\widetilde{W}^T(t) = d\widetilde{W}(t) - \psi^T(t)$$

is a $\mathbb{Q}^T$ standard Brownian motion. Then,

$$\begin{aligned}&dx(t) = -ax(t)dt + \sigma(t)dW_1(t) = -ax(t)dt + \sigma(t)d\widetilde{W}_1(t) \\ &= -ax(t)dt+\sigma(t)\left[d\widetilde{W}_1^T(t) - \sigma(t)\left(\frac{1-e^{-a(T-u)}}{a}\right)dt - \rho\eta(t)\left(\frac{1-e^{-b(T-u)}}{b}\right)dt\right] \\ &= \left[-ax(t) - \sigma(t)^2\left(\frac{1-e^{-a(T-t)}}{a}\right) - \rho\eta(t)\sigma(t)\left(\frac{1-e^{-b(T-t)}}{b}\right)\right]dt+\sigma(t)d\widetilde{W}_1^T(t)\end{aligned}$$

and also

$$\begin{aligned}&dy(t) = -by(t)dt+\eta(t)dW_2(t) = -by(t)dt+\rho\eta(t)d\widetilde{W}_1(t)+\sqrt{1-\rho^2}\eta(t)d\widetilde{W}_2(t) \\ &= -by(t)dt+\rho\eta(t)\left[d\widetilde{W}_1^T(t) - \sigma(t)\left(\frac{1-e^{-a(T-u)}}{a}\right)dt - \rho\eta(t)\left(\frac{1-e^{-b(T-u)}}{b}\right)dt\right] \\ &\qquad + \sqrt{1-\rho^2}\eta(t)\left[d\widetilde{W}_2^T(t) - \sqrt{1-\rho^2}\ \eta(t)\left(\frac{1-e^{-b(T-u)}}{b}\right)dt\right] \\ &\qquad = \left[-by(t) - \rho\sigma(t)\eta(t)\left(\frac{1-e^{-a(T-u)}}{a}\right) - \rho^2\eta^2(t)\left(\frac{1-e^{-b(T-u)}}{b}\right)\right. \\ &\left. - \left(1-\rho^2\right)\eta^2(t)\left(\frac{1-e^{-b(T-u)}}{b}\right)\right]dt + \rho\eta(t)d\widetilde{W}_1^T(t) + \sqrt{1-\rho^2}\eta(t)d\widetilde{W}_2^T(t) \\ &\qquad = \left[-by(t) - \eta^2(t)\left(\frac{1-e^{-b(T-u)}}{b}\right) - \rho\sigma(t)\eta(t)\left(\frac{1-e^{-a(T-u)}}{a}\right)\right]dt \\ &\qquad\qquad + \rho\eta(t)d\widetilde{W}_1^T(t) + \sqrt{1-\rho^2}\eta(t)d\widetilde{W}_2^T(t)\end{aligned}$$

The dynamics is equivalent to

$$\begin{aligned}dx(t) = &\left[-ax(t) - \sigma(t)^2\left(\frac{1-e^{-a(T-t)}}{a}\right) - \rho\eta(t)\sigma(t)\left(\frac{1-e^{-b(T-t)}}{b}\right)\right]dt \\ &+ \sigma(t)dW_1^T(t)\end{aligned}$$



Electronic copy available at: https://ssrn.com/abstract=3598285

$$dy(t) = \left[-by(t) - \eta(t)^2 \left(\frac{1-e^{-b(T-t)}}{b}\right) - \rho\eta(t)\sigma(t) \left(\frac{1-e^{-a(T-t)}}{a}\right)\right] dt + \eta(t) dW_2^T(t)$$

where $W^T(t) = (W_1^T(t), W_2^T(t))'$ is a 2-dimensional $\mathbb{Q}^{\mathbb{T}}$ Brownian motion with instantaneous correlation equal to $\rho$. □

## A.4 The forward dynamics of $x(t)$ and $y(t)$ (proposition 6)

*Proof.* We will limit ourselves to the calculations for $x(t)$. Multiplying both sides by $e^{at}$ gives

$$d\left(e^{at}x(t)\right) = e^{at}\left[-\sigma(t)^2 \left(\frac{1-e^{-a(T-t)}}{a}\right) - \rho\eta(t)\sigma(t) \left(\frac{1-e^{-b(T-t)}}{b}\right)\right] dt + \sigma(t)e^{at} dW_1^T(t)$$

Then, conditional on $\mathcal{F}_s$,

$$x(t) = e^{-a(t-s)}x(s) + \int_s^t \sigma(u)e^{-a(t-u)} dW_1^T(u) - \int_s^t e^{-a(t-u)}\left[\sigma(u)^2 \left(\frac{1-e^{-a(T-u)}}{a}\right) + \rho\eta(u)\sigma(u) \left(\frac{1-e^{-b(T-u)}}{b}\right)\right] du$$

If we denote the last integral by $M_x^T(s,t)$, we have that

$$x(t) = e^{-a(t-s)}x(s) - M_x^T(s,t) + \int_s^t \sigma(u)e^{-a(t-u)} dW_1^T(u)$$



Electronic copy available at: https://ssrn.com/abstract=3598285

Now, performing the calculations for $M_x^T(s,t)$ yields

$$\begin{aligned}
&\int_s^t \left[ e^{-a(t-u)}\sigma(u)^2 \left( \frac{1-e^{-a(T-u)}}{a} \right) + \rho\eta(u)\sigma(u)e^{-a(t-u)} \left( \frac{1-e^{-b(T-u)}}{b} \right) \right] du \\
&= \sum_{i=i(s)}^{i(t)} \int_{\max(s,t_{i-1})}^{\min(t,t_i)} \left[ \sigma_{i-1}^2 e^{-a(t-u)} \left( \frac{1-e^{-a(T-u)}}{a} \right) + \rho\eta_{i-1}\sigma_{i-1}e^{-a(t-u)} \left( \frac{1-e^{-b(T-u)}}{b} \right) \right] du \\
&\qquad = \sum_{i=i(s)}^{i(t)} \left\{ \sigma_{i-1}^2 \left[ \frac{e^{-a(t-\min(t,t_i))} - e^{-a(t-\max(s,t_{i-1}))}}{a^2} \right.\right. \\
&\qquad\qquad \left. - \frac{e^{-a(t+T-2\min(t,t_i))} - e^{-a(t+T-2\max(s,t_{i-1}))}}{2a^2} \right] \\
&\qquad\qquad + \rho\eta_{i-1}\sigma_{i-1} \left[ \frac{e^{-a(t-\min(t,t_i))} - e^{-a(t-\max(s,t_{i-1}))}}{ab} \right. \\
&\qquad\qquad \left.\left. - \frac{e^{-at-bT+(a+b)\min(t,t_i)} - e^{-at-bT+(a+b)\max(s,t_{i-1})}}{b(a+b)} \right] \right\} \\
&\qquad = \sum_{i=i(s)}^{i(t)} \left[ \left( \frac{\sigma_{i-1}^2}{a^2} + \rho\frac{\eta_{i-1}\sigma_{i-1}}{ab} \right) \left( e^{-a(t-\min(t,t_i))} - e^{-a(t-\max(s,t_{i-1}))} \right) \right. \\
&\qquad\qquad - \frac{\sigma_{i-1}^2}{2a^2} \left( e^{-a(t+T-2\min(t,t_i))} - e^{-a(t+T-2\max(s,t_{i-1}))} \right) \\
&\qquad\qquad \left. - \frac{\rho\eta_{i-1}\sigma_{i-1}}{b(a+b)} \left( e^{-at-bT+(a+b)\min(t,t_i)} - e^{-at-bT+(a+b)\max(s,t_{i-1})} \right) \right]
\end{aligned}$$

Introducing

$$\Delta T_i^{(l)} = T - \max(s, t_{i-1}), \qquad \Delta T_i^{(r)} = T - \min(t, t_i)$$

concludes the proof. □



Electronic copy available at: https://ssrn.com/abstract=3598285

# References


[1] Tomas Bjork. *Arbitrage Theory in Continuous Time, third edition.* 2009.

[2] Mario Bonino and Riccardo Casalini. Benchmarking interest rate models. *http://ssrn.com/abstract=3403529*, 2019.

[3] Damiano Brigo and Fabio Mercurio. *Interest Rate Models — Theory and Practice. With Smile, Inflation and Credit.* 2006.

[4] Mercurio F. Brigo D. Displaced and mixture diffusions for analytically-tractable smile models. *Geman H., Madan D., Pliska S.R., Vorst T. (eds) Mathematical Finance, Bachelier Congress 2000. Springer Finance. Springer, Berlin, Heidelberg*, 2002.

[5] Darrell Duffie and Kenneth J. Singleton. Modeling term structures of defaultable bonds. *Review of Financial Studies*, 1999.

[6] Bruno Dupire. Pricing with a smile. *Risk*, pages Jan. 18–20, 1994.

[7] Anna Maria Gambaro, Riccardo Casalini, Gianluca Fusai, and Alessandro Ghilarducci. Quantitative assessment of common practice procedures in the fair evaluation of embedded options in insurance contracts. *Insurance: Mathematics and Economics*, Volume 81:Pages 117–129, 2018.

[8] Anna Maria Gambaro, Riccardo Casalini, Gianluca Fusai, and Alessandro Ghilarducci. A market-consistent framework for the fair evaluation of insurance contracts under solvency ii. *Decisions in Economics and Finance*, Issue 1/2019, 2019.

[9] Patrick S. Hagan, Deep Kumar, Andrew S. Lesniewski, and Diana E. Woodward. Managing smile risk. *Wilmott magazine*, pages Jul. 84–108, 2002.

[10] S. L. Heston. A closed-form solution for options with stochastic volatility and applications to bond and currency options. *Review of Financial Studies*, 1993.

[11] John Hull and Alan White. Pricing interest rate derivative securities. *Review of Financial Studies*, 1990.

[12] Y. Perl, A. Itai, and H. Havni. Interpolation search. a log logn search. *Communication of the ACM*, 1978.




Electronic copy available at: https://ssrn.com/abstract=3598285

[13] Oldrich Vasicek. An equilibrium characterization of the term structure. *Journal of Financial Economics, 5, 177-188*, 1977.



Electronic copy available at: https://ssrn.com/abstract=3598285